Commun. Comput. Phys.
doi: 10.4208/cicp.2014.m424

Vol. **17**, No. 4, pp. 1007-1018
April 2015

A Finite-Difference Lattice Boltzmann Approach for Gas Microflows

G. P. Ghiroldi and L. Gibelli*

Dipartimento di Scienze e Tecnologie Aerospaziali, Via la Masa 34, Politecnico di Milano, 20156 Milano, Italy.

Received 26 January 2014; Accepted (in revised version) 7 April 2014

Abstract. Finite-difference Lattice Boltzmann (LB) models are proposed for simulating gas flows in devices with microscale geometries. The models employ the roots of half-range Gauss-Hermite polynomials as discrete velocities. Unlike the standard LB velocity-space discretizations based on the roots of full-range Hermite polynomials, using the nodes of a quadrature defined in the half-space permits a consistent treatment of kinetic boundary conditions. The possibilities of the proposed LB models are illustrated by studying the one-dimensional Couette flow and the two-dimensional square driven cavity flow. Numerical and analytical results show an improved accuracy in finite Knudsen flows as compared with standard LB models.

PACS: 47.11.-j, 47.45.-n, 47.61.-k

Key words: Lattice Boltzmann models, half-range Hermite polynomials, kinetic boundary conditions.

1 Introduction

The outgrowing development of microelectromechanical systems (MEMS) has spurred interest in studying gas flows in devices with microscale geometries. These flows, which are referred to as gas microflows, are usually distinguished by relatively large Knudsen numbers and small Mach numbers. Because of the large Knudsen numbers, the conventional hydrodynamic approach breaks down and a description based on the Boltzmann equation is required [1]. Numerical evidence from full solutions of the Boltzmann equation suggests that accurate results for isothermal flows can also be determined by simpler kinetic model equations such as the one proposed by Bathnagar, Gross and Krook and, independently, by Welander (BGKW) [1]. Therefore it is a common practice to model

*Corresponding author. *Email addresses:* gian.ghiroldi@mail.polimi.it (G. P. Ghiroldi), livio.gibelli@polimi.it (L. Gibelli)

 ©2015 Global-Science Press

https://doi.org/10.4208/cicp.2014.m424 Published online by Cambridge University Press

isothermal gas microflows by the BGKW kinetic model equation and, due to the small Mach numbers, to linearize it around the equilibrium state [2]. Numerous studies on gas microflows based on the numerical solution of the linearized BGKW kinetic model equation [3–5] and/or the linearized Boltzmann equation [6] have been reported over the years. Recently, the Lattice Boltzmann (LB) method has attracted considerable interest as an alternative tool for studying gas flows in microfluidic devices [7–14]. Although it was evolved from lattice-gas cellular automaton models for mimicking the Navier-Stokes hydrodynamics, the LB method can potentially describe gas microflows since it can be viewed as the discrete ordinate method to solve the linearized BGKW kinetic model equation [15,16]. Within the framework of single relaxation time modeling, several high-order LB models have been developed in the attempt to adequately reproduce the non equilibrium effects of finite Knudsen flows, such as the velocity slip at the solid walls and the nonlinear stress-strain relationship within the Knudsen layer [17,18]. Some models have been derived by using a local mean free path in order to account for the presence of solid surfaces [7]. Although this approach has been shown to be effective in many applications, it is phenomenological in nature and, as such, not perfectly general. Composite models have also been developed which result from the superposition of discrete velocities determined from odd and even quadrature formula [9]. However, the most common strategy is using a greater number of discrete velocities determined from a full-range Gauss-Hermite quadrature [8, 11, 12], possibly adopting a multiscale approach to contain the increase in the computational cost [10]. However, more discrete velocities do not guarantee an improved accuracy because of the quadrature error in dealing with the boundary conditions [13]. As a matter of fact, abscissae of the full-range Gauss-Hermite quadrature schemes are derived to obtain accurate evaluation of the moments of the distribution function defined over the entire velocity space. In contrast, they provide only an approximately estimate of the half-range integrals that enter in the formulation of kinetic boundary conditions [19].

The present work aims at showing that the capability of standard finite-difference LB models to describe finite Knudsen gas flows can be improved by using weights and nodes as given by the half-range Gauss-Hermite quadrature [20]. This velocity space discretization permits to explicitly account for the discontinuity of the distribution function at the solid walls and therefore leads to a faster convergence rate of the numerical solution. In kinetic theory applications, the importance of a consistent treatment of boundary conditions has been recognized as early as the sixties of the past century [21] and the half-range discrete ordinate method has been widely used since then [22–26]. However to the authors' knowledge, no previous works have explicitly shown that the quadrature based on half-range Hermite polynomials can easily address the issue of boundary conditions for the LB simulations of gas microflows [13]. As a matter of fact, although it is well known that finite-difference LB models can be developed from different quadrature formula [27], most of the high-order LB models applied to simulate gas flows in microchannels use the roots of full-range Hermite polynomials as discrete velocities [7–13]. In Ref. [19] it was observed that an improved accuracy in dealing with boundary conditions can be achieved

https://doi.org/10.4208/cicp.2014.m424 Published online by Cambridge University Press

by using quadrature formula defined in the half-space. However, this possibility was not further developed because of the mismatch between the nodes of the quadrature used at the boundary and those in the bulk. In the present work, however, the nodes of half-range Gauss-Hermite quadrature formula are used in the whole domain. It is worth pointing out that the validity of this velocity space discretization is not restricted to planar surfaces but it also holds in the presence of sharp corners. Moreover, by making use of a body fitted coordinate system, curvilinear geometries can be handled as well [28]. Let us mention that LB models have been recently developed which are based on the spherical coordinate system in the velocity space [29]. These models can also provide a consistent treatment of kinetic boundary conditions and they thus constitute an alternative approach which is especially interesting for dealing with boundary value problems in domains with complex geometry. The rest of the paper is organized as follows. Section 2 presents the finite-difference LB models used in the present study. They differ from standard finite-difference LB models only in that weights and nodes are provided by the half-range Gauss-Hermite quadrature formula. Section 3 shows the improved accuracy offered by the proposed approach when applied to two classical finite Knudsen boundary driven problems, namely the Couette flow and the square driven cavity flow. Finally, Section 4 summarizes the main results and the future research directions.

2 Finite-difference Lattice Boltzmann (LB) models

In the absence of external force fields and by using the same notation as in Ref. [12], the non dimensional form of LB models reads

$$\frac{\partial f_\alpha}{\partial t}+\boldsymbol{\xi}_\alpha\cdot\nabla f_\alpha=-\frac{1}{\mathrm{Kn}}\left(f_\alpha-f_\alpha^{(eq)}\right), \tag{2.1}$$

where the Knudsen number is defined as $\mathrm{Kn}=\mu_0\sqrt{RT_0}/(p_0 l)$ with μ_0,T_0,p_0 the reference gas viscosity, temperature and pressure, respectively, l a characteristic length and

$$f_\alpha(\boldsymbol{r},t)=w_\alpha f(\boldsymbol{r},\boldsymbol{\xi}_\alpha,t)/\omega(\boldsymbol{\xi}_\alpha), \tag{2.2}$$

$$f_\alpha^{(eq)}(\boldsymbol{r},t)=w_\alpha f^{(eq)}(\boldsymbol{r},\boldsymbol{\xi}_\alpha,t)/\omega(\boldsymbol{\xi}_\alpha), \tag{2.3}$$

where

$$\omega(\boldsymbol{\xi})=\frac{1}{(2\pi)^{d_v/2}}\exp\left(-\frac{\xi^2}{2}\right). \tag{2.4}$$

In Eqs. (2.2) and (2.3), f is the distribution function, $f^{(eq)}$ is the d_v-dimensional equilibrium Maxwellian and $w_\alpha,\boldsymbol{\xi}_\alpha$ are the n weights and nodes determined from a quadrature formula, respectively [27]. Since we are considering isothermal flows, the terms related to the temperature in the second-order approximation of the equilibrium Maxwellian can be disregarded and $f^{(eq)}$ can thus be written as

$$f^{(eq)}(\boldsymbol{r},t)=\omega(\boldsymbol{\xi})\rho(\boldsymbol{r},t)\left[1+\boldsymbol{\xi}\cdot\boldsymbol{u}(\boldsymbol{r},t)\right], \tag{2.5}$$

https://doi.org/10.4208/cicp.2014.m424 Published online by Cambridge University Press

where ρ and $\boldsymbol{u}$ are the density and macroscopic velocity, respectively, which can be computed by sums over the discrete velocity set

$$\rho(\boldsymbol{r},t)=\sum_{\alpha=1}^{n} f_\alpha(\boldsymbol{r},t), \tag{2.6}$$

$$\rho(\boldsymbol{r},t)\boldsymbol{u}(\boldsymbol{r},t)=\sum_{\alpha=1}^{n} \boldsymbol{\xi}_\alpha f_\alpha(\boldsymbol{r},t). \tag{2.7}$$

Likewise, boundary conditions can be derived by a direct discretization of Maxwell's diffuse-specular scattering kernel [19, 30, 31]. For the sake of simplicity, let us consider a plane wall at $y=0$ with reference temperature and constant velocity u_w in the positive x-direction. Let us further suppose that the gas fills the half space $y>0$ and molecules which strike the wall are re-emitted according to Maxwell's scattering kernel with complete accommodation. The discrete form of the kinetic boundary condition at a point $\boldsymbol{r}_w$ of the solid surfaces reads

$$f_\alpha(\boldsymbol{r}_w,t)=w_\alpha\rho_w(\boldsymbol{r}_w,t)\,(1+\xi_{x,\alpha}u_w), \quad \xi_{y,\alpha}>0. \tag{2.8}$$

In Eq. (2.8), ρ_w can be obtained through the impermeability condition, which states that the normal component of the gas velocity on the wall vanishes

$$\rho_w(\boldsymbol{r}_w,t)=-(2\pi)^{1/2}\sum_{\xi_{y,\alpha}<0} \xi_{y,\alpha} f_\alpha(\boldsymbol{r}_w,t). \tag{2.9}$$

The models, Eq. (2.1), as well as the kinetic boundary conditions, Eqs. (2.8) and (2.9), used in the present work, differ from standard finite-difference LB models only in that weights and nodes are given by the half-range Gauss-Hermite quadrature. These are reported in Table 1 for the one-dimensional case, being higher order quadratures obtained from the tensor product of the corresponding one-dimensional quadrature. Following standard terminology, we denote by D_mQ_n the m dimensional LB models with n discrete velocities, using h as superscript of Q if weights and nodes are defined based on the half-range Gauss-Hermite quadrature formula. Notice should be made that the roots of half-range Hermite polynomials are irrational and therefore the resulting fully-discrete numerical scheme is computationally more demanding than the simpler "stream-and-collide" algorithm. The exact space discretization of the advection step of on-lattice LB models is therefore no longer possible and the potential high efficiency of its parallel implementation is partially lost. However, off-lattice schemes may offer some advantages such as improved accuracy and enhanced geometrical flexibility [32]. The use of high performance computing is still feasible but the porting of algorithms involving finite-difference approximations certainly requires some additional effort [33]. It is worth noticing that an important correspondence can be identified between the approach developed in the present work and the moment method presented in Ref. [24] for studying gas microflows.

https://doi.org/10.4208/cicp.2014.m424 Published online by Cambridge University Press

Table 1: Nodes, ξ_α, and weights, w_α, of the one-dimensional half-range Gauss-Hermite quadrature.

Quadrature	ξ_α	w_α
$D_1Q_4^h$	∓ 0.4245383286	0.3613798911
	∓ 1.77119083	0.1386201089
$D_1Q_6^h$	∓ 0.2694842630	0.2516453504
	∓ 1.199609295	0.2236832664
	∓ 2.545268446	0.0246713831
$D_1Q_8^h$	∓ 0.1891884657	0.1835325640
	∓ 0.8829284442	0.2375842404
	∓ 1.898635201	0.07528686870
	∓ 3.199890790	0.003596326913

There, the isothermal linearized BGKW kinetic model equation has been solved by expanding the distribution function as a series of half-range Hermite polynomials. Expansion coefficients are the moments of the distribution function which, in turn, are strictly related to the macroscopic quantities. By using the half-range Gauss-Hermite quadrature formula for evaluating these integrals, a one-to-one correspondence can be identified between the expansion coefficients and the values of the distribution function at the roots of half-range Hermite polynomials. The two approaches are therefore equivalent even though the formulation which is here adopted is computationally more efficient.

3 Numerical results

We demonstrate that the proposed approach can be used to simulate gas microflows by studying two classical driven boundary value problems, i.e., the Couette and the cavity flows. Both problems are regarded as two-dimensional and the driven velocity, u_w, is assumed sufficiently low so that the gas flow can be considered in the linearized regime [34]. Fig. 1 illustrates the flow geometry for both problems. Analytical and numerical solutions of the proposed finite-difference LB models are then compared with the numerical predictions of the linearized BGKW kinetic model equation. Numerical solutions of Eq. (2.1) have been determined by a first-order time splitting of the evolution operator and by combining a first-order explicit upwind scheme for the transport step with a first-order explicit Euler scheme for the relaxation step. More sophisticated methods should be used for both coupling and solving transport and relaxation steps if a more accurate and efficient numerical scheme is needed [35]. However, the main aim of the present work is to show that an improved accuracy in describing finite Knudsen flows can be achieved by using the roots of half-range Hermite polynomials as discrete velocities. This has been assessed by running the same numerical code twice, once with nodes and weights as given by full-range Gauss-Hermite quadrature and once with nodes and weights as given by half-range Gauss-Hermite quadrature. The validity of this compar-

https://doi.org/10.4208/cicp.2014.m424 Published online by Cambridge University Press

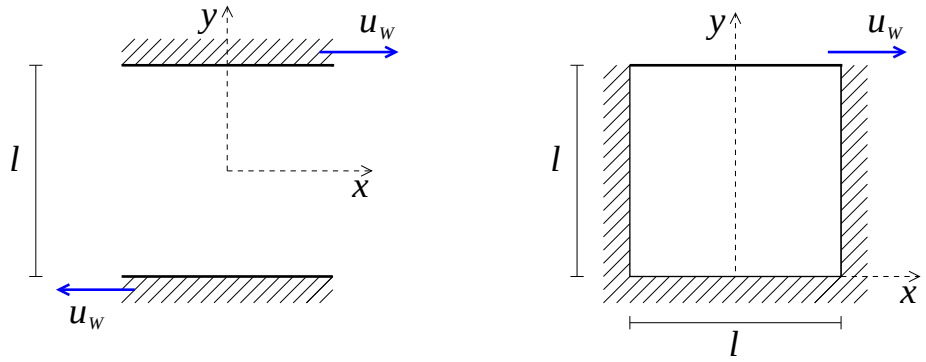


Figure 1: Flow geometry. Couette problem (left panel). Square cavity problem (right panel).

ison is therefore independent on the numerical scheme that has been used to solve the discrete kinetic equation.

3.1 Couette flow

The Couette flow problem is depicted in the left panel of Fig. 1. The upper plate moves in the positive x-direction with a velocity u_w and the lower plate moves with a velocity $-u_w$. The two plates are separated by the distance l. Diffuse boundary conditions have been implemented at the plates and periodic boundary conditions have been utilized at opposite ends of the channels. It is worth noticing that the proposed models employ the quadrature nodes of the positive and negative half-range Gauss-Hermite quadrature formula as discrete velocities both in the x- and y-directions. However numerical computations showed that the same results are obtained if the x-direction of the velocity space is discretized by using the roots of full-range Hermite polynomials. By proceeding as in Ref. [24], it is not difficult to obtain a closed-form solution of the $D_2Q_{16}^h$ model for the stationary planar Couette flow

$$\frac{u_x(y/l)}{u_w}=\frac{\left[\sinh\left(\frac{0.9494}{\mathrm{Kn}}\right)+0.7978\cosh\left(\frac{0.9404}{\mathrm{Kn}}\right)\right]\frac{y}{l}+0.5642\mathrm{Kn}\sinh\left(\frac{1.881}{\mathrm{Kn}}\frac{y}{l}\right)}{(0.7071\mathrm{Kn}+0.3989)\cosh\left(\frac{0.9404}{\mathrm{Kn}}\right)+(1.128\mathrm{Kn}+0.5)\sinh\left(\frac{0.9404}{\mathrm{Kn}}\right)}, \tag{3.1}$$

$$\frac{\sqrt{RT_0}p_{xy}}{u_w p_0}=-\mathrm{Kn}\frac{\sinh\left(\frac{0.9494}{\mathrm{Kn}}\right)+0.7979\cosh\left(\frac{0.9404}{\mathrm{Kn}}\right)}{(0.7071\mathrm{Kn}+0.3989)\cosh\left(\frac{0.9404}{\mathrm{Kn}}\right)+(1.128\mathrm{Kn}+0.5)\sinh\left(\frac{0.9404}{\mathrm{Kn}}\right)}. \tag{3.2}$$

Beside their intrinsic interest, Eqs. (3.1) and (3.2), as well as a similar closed-form solution obtained in Ref. [36] for the D_2Q_{16} model, are of practical importance in that they permit to validate the numerical code. Figs. 2 and 3 show the velocity slip, $1-u_x/u_w$, at the upper plate and the ratio between the xy-component of the stress tensor, p_{xy}, and the value of the pressure in the free molecular regime, $p_{fm}=-2p_0u_w/\sqrt{\pi RT_0}$, versus the Knudsen

https://doi.org/10.4208/cicp.2014.m424 Published online by Cambridge University Press

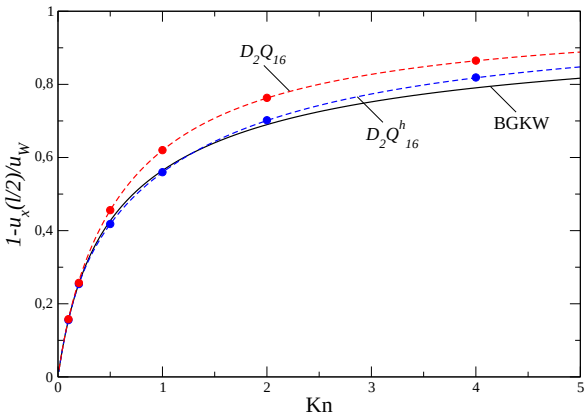


Figure 2: Couette flow: Velocity slip at the upper plate versus the Knudsen number.

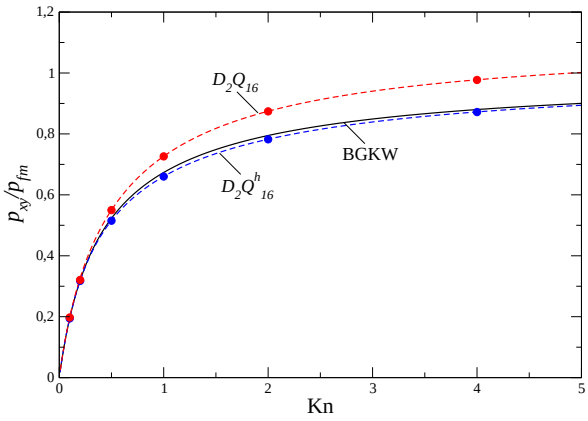


Figure 3: Couette flow: Reduced xy-component of the stress tensor versus the Knudsen number.

number, Kn, respectively. Both figures use the same conventions. Solid line are the solutions of the linearized BGKW kinetic model equation obtained by means of the moment method described in Ref. [24] and assessed against classical results obtained in Refs. [37] and [38]. Dashed lines are the closed-form solutions of the $D_2Q^h_{16}$ model, as given by Eqs. (3.1) and (3.2) evaluated at $y/l=1/2$, and of the D_2Q_{16} model, which is reported in Ref. [36]. Solid circles are the numerical solutions of the $D_2Q^h_{16}$ and D_2Q_{16} models. Only even-order LB models have been considered since they perform significantly better than those with an odd-order quadrature no matter how the order is [8, 11]. As it is clearly shown, although the same number of discrete velocities is employed, the $D_2Q^h_{16}$ model gives much improved results as compared with standard D_2Q_{16} model. The prediction of the velocity slip shows a very good match with the results obtained by solving the linearized BGKW kinetic model equation not only in the continuum and slip flow regimes but also in the early transition regime. The xy-component of the stress tensor shows a

https://doi.org/10.4208/cicp.2014.m424 Published online by Cambridge University Press

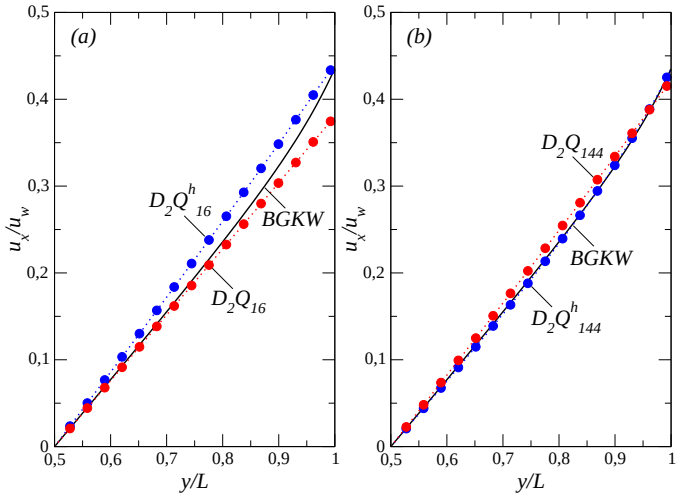


Figure 4: Couette flow: Nondimensional velocity profile through the half-channel. Kn = 1. (a) $n = 16$, (b) $n = 144$.

quite good agreement even in a wider range of Knudsen numbers. Convergence of the results at Kn = 1 with increasing number of discrete velocities is reported in Fig. 4 for the velocity profile. Solid line is the solution of the linearized BGKW kinetic model equation obtained by means of the moment method described in Ref. [24]. Dotted lines with solid circles are the numerical solutions obtained by using $n = 16$ (left panel) and $n = 144$ (right panel) discrete velocities, respectively. The D_2Q_{16} model provides a slightly better description of the gas behavior in the bulk of the flow than the $D_2Q^h_{16}$ model. A possible explanation is that the full-range Gauss-Hermite quadrature with $n = 16$ discrete velocities integrates exactly continuous polynomials of order five in each velocity component whereas the half-range Gauss-Hermite quadrature with the same number of nodes integrates exactly linear polynomials with a possible discontinuity at the origin. It is thus reasonable that the former can be more accurate in the bulk of the flow where the distribution function is continuous whereas the latter can perform better close to the solid surface where the distribution function is expected to be discontinuous. Nevertheless, as the results with $n = 144$ clearly show, using the roots of half-range Hermite polynomials as discrete velocities greatly speed-up the convergence to the kinetic theory solution. A similar analysis for the xy-component of the stress tensor shows that the numerical prediction of the $D_2Q^h_{16}$ model at Kn = 1 is affected by a relative error which is lower than 5% whereas at least 12 nodes per each velocity component should be used for the standard high-order LB models to achieve the same level of accuracy.

3.2 Square driven cavity flow

The square driven cavity flow is depicted in the right panel of Fig. 1. All the walls are the same length l and isothermal. The flow is driven by the uniform translation of the

https://doi.org/10.4208/cicp.2014.m424 Published online by Cambridge University Press

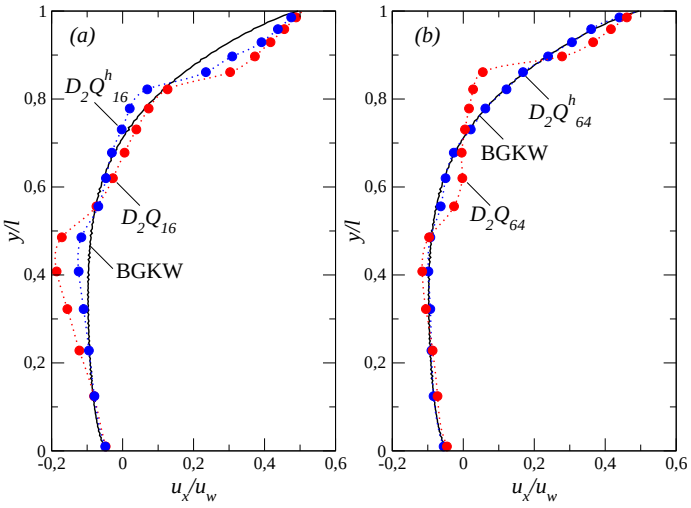


Figure 5: Cavity flow: Profile of the nondimensional horizontal component of the mean velocity crossing the center of the cavity. Kn = 0.4. (a) $n = 16$, (b) $n = 64$.

top with a velocity u_w in the positive x-direction. Diffuse boundary conditions have been implemented at the walls [39]. Numerical simulations have been carried out for Knudsen numbers in the range $[0.05,0.4]$. This problem constitutes a severe test to assess the capability of the proposed velocity space discretization to describe the gas behavior in complex geometries. Indeed, the discontinuities which exist at the four corners, particularly the two at the top, propagate inside the computational domain and might cause the quadrature to fail. Since the discontinuities decay with distance owing to molecular collisions, it is expected that these numerical problems become more severe as the Knudsen number is increased. In Fig. 5, the profile of the nondimensional horizontal component of the macroscopic velocity, u_x/u_w, crossing the center of the cavity are thus shown for the higher Knudsen number, Kn = 0.4. Solid line is the solution of the linearized BGKW equation obtained with the numerical method described in Ref. [39]. Dotted lines with solid circles are the numerical solutions provided by full- and half-range LB models with $n = 16$ (left panel) and $n = 64$ (right panel) discrete velocities. As it was clearly shown, both methods suffer from an unphysical oscillatory behavior due to the difficulty of the quadratures to evaluate a region where discontinuities are present. Although more sophisticated methods can be adopted [39], we here simply notice that the problem can be overcome by a reasonable increase in the number of discrete velocities. As for the case of the Couette flow, the proposed approach shows better convergence properties. For instance, the errors in the $\mathcal{L}^1$-norm of full- and half-range LB models using $n = 16$ discrete velocities are 0.0445 and 0.0280, respectively, and reduce to 0.0218 and 0.00354 for $n = 64$. Table 2 reports a comparison of the values of the mean dimensionless shear stress along the moving plate, D, and the dimensionless flow rate of the main vortex, G, obtained by the different models [39]. The predictions of the $D_2Q^h_{16}$ model show a better agreement

https://doi.org/10.4208/cicp.2014.m424 Published online by Cambridge University Press

Table 2: Cavity flow: Drag coefficient, D, and reduced flow rate, G, versus the Knudsen number.

	D			G		
Kn	BGKW	$D_2Q_{16}^h$	D_2Q_{16}	BGKW	$D_2Q_{16}^h$	D_2Q_{16}
0.05	0.258	0.256	0.270	0.154	0.153	0.162
0.1	0.328	0.327	0.350	0.136	0.128	0.153
0.2	0.425	0.417	0.467	0.121	0.109	0.148
0.4	0.385	0.384	0.421	0.110	0.0961	0.145

with the kinetic theory results than those of the D_2Q_{16} model. In spite of the unphysical oscillations which affect the macroscopic velocity, the drag coefficient converges up to two significant figures. Instead the error in the reduced flow rate is less than 1% for Kn$=$0.05 but rapidly increases for greater Knudsen numbers. However, as expected from Ref. [24], a quite good agreement can be found up to Kn$=10$ if the $D_2Q_{36}^h$ model is used.

4 Conclusion

We have shown that, in comparison with full-range finite-difference high-order LB models, using the nodes of half-range Gauss-Hermite quadrature as discrete velocities permits to consistently deal with kinetic boundary conditions and thus to achieve a more accurate description of the gas behavior close to solid surfaces. Applications to one- and two-dimensional driven boundary value problems show that, even using a small number of discrete velocities, accurate results can be obtained in a wide range of Knudsen numbers which extends up to the early transition regime. The proposed approach is also of interest in that, as it can be deduced from Ref. [24], half-range LB models with N discrete velocities simplify to full-range LB models with $N/2^{d_s}$ velocities far away from solid surfaces, being d_s the dimension of the physical space. This suggests the development of a hybrid approach which combines the capability of half-range LB models to accurately describe the gas behavior in the Knudsen layers with the higher computational efficiency of full-range LB models when applied to the bulk of the gas.

Acknowledgments

The authors would like to thank Prof. A. Frezzotti for critically reading the paper and Prof. D. Valougeorgis for providing his numerical code. This work has been partly supported by "Progetto Giovani Ricercatori GNFM 2013", Regione Lombardia and CILEA Consortium through a LISA Initiative (Laboratory for Interdisciplinary Advanced Simulation) 2011 grant [link: `http://lisa.cilea.it`].

https://doi.org/10.4208/cicp.2014.m424 Published online by Cambridge University Press

References

[1] C. Cercignani, The Boltzmann equation and its applications, Springer-Verlag, New York, 1988.
[2] G. E. Karniadakis, A. Beskok and A. Narayan, Microflows and nanoflows: Fundamentals and simulation, Springer, Berlin, 2005.
[3] S. Lorenzani, L. Gibelli, A. Frangi and C. Cercignani, Kinetic approach to gas flows in microchannels, Nano. Micro. Therm. Eng., 11 (1-2) (2007), 211-226.
[4] S. Naris and D. Valougeorgis, Boundary-driven nonequilibrium gas flow in a grooved channel via kinetic theory, Phys. Fluids, 19 (2007), 067103.
[5] A. Alexeenka, S. Chigullapalli, J. Zeng, X. Guo, A. Kovacs and D. Peroulis, Uncertainty in microscale gas damping: Implications on dynamics of capacitive MEMS switches, Reliab. Eng. Syst. Safe., 96 (2011), 1171-1183.
[6] C. Cercignani, A. Frangi, A. Frezzotti, G. P. Ghiroldi, L. Gibelli and S. Lorenzani, On the application of the Boltzmann equation to the simulation of fluid structure interaction in MEMS, Sens. Lett., 6 (2008), 121-129.
[7] Y. H. Zhang, X. J. Gu, R. W. Barber and D. R. Emerson, Capturing Knudsen layer phenomena using a lattice Boltzmann model, Phys. Rev. E., 74 (2006), 046704-7.
[8] S. H. Kim, H. Pitsch and I. D. Boyd, Accuracy of higher-order lattice Boltzmann methods for microscale flows with finite Knudsen numbers, J. Comput. Phys., 227 (2008), 8655-8671.
[9] L. de Izarra, J. L. Rouet and B. Izrar, High-order lattice Boltzmann models for gas flow for a wide range of Knudsen numbers, Phys. Rev. E, 84 (2011), 066705.
[10] J. Meng, Y. Zhang and X. Shan, Multiscale lattice Boltzmann approach to modeling gas flows, Phys. Rev. E, 83 (2011), 046701.
[11] J. Meng and Y. Zhang, Accuracy analysis of high-order lattice Boltzmann models for rarefied gas flows, J. Comput. Phys., 230 (2011), 835-849.
[12] J. Meng and Y. Zhang, Gauss-Hermite quadratures and accuracy of lattice Boltzmann models for nonequilibrium gas flows, Phys. Rev. E, 83 (2011), 036704.
[13] Y. Shi, P. L. Brookes, Y. W. Yap and J. E. Sader, Accuracy of the lattice Boltzmann method for low-speed noncontinuum flows, Phys. Rev. E, 83 (2011), 045701(R).
[14] Z. Xu and Z. Guo, Pressure distribution of the gaseous flow in microchannel: A lattice Boltzmann study, Commun. Comput. Phys., 14 (2013), 1058-1072.
[15] X. He and L. S. Luo, Theory of the lattice Boltzmann method: From the Boltzmann equation to the lattice Boltzmann equation, Phys. Rev. E, 56 (1997), 6811-6817.
[16] X. Shan and X. He, Discretization of the velocity space in the solution of the Boltzmann equation, Phys. Re. Lett., 80 (1998), 65-68.
[17] D. A. Lockerby and J. Reese, On the modelling of isothermal gas flows at the microscale, J. Fluid Mech., 604 (2008), 235-261.
[18] W. Zhang, G. Meng and X. Wei, A review on slip models for gas microflows, Microfluid. Nanofluid., 13 (2012), 845-882.
[19] S. Ansumali and I. V. Karlin, Kinetic boundary conditions in the lattice Boltzmann method, Phys. Rev. E., 66 (2002), 026311.
[20] B. D. Shizgal, A Gaussian quadrature procedure for use in the solution of the Boltzmann equation and related problems, J. Comput. Phys., 41 (1981), 309-328.
[21] E. P. Gross, E. A. Jackson and S. Ziering, Boundary value problems in kinetic theory of gases, Ann. Phys., 1 (1957), 141-167.
[22] A. B. Huang and D. P. Giddens, The discrete ordinate method for the linearized boundary

https://doi.org/10.4208/cicp.2014.m424 Published online by Cambridge University Press

value problems in kinetic theory of gases, 5th Int. Symp. on Rarefied Gas Dynamics, (1967), 481-504.
[23] L. B. Barichello, M. Camargo, P. Rodrigues, and C. E. Siewert, Unified Solutions to Classical Flow Problems Based on the BGK Model, ZAMP, 52 (2001), 517-534.
[24] A. Frezzotti, L. Gibelli and B. Franzelli, A moment method for low speed flows, Cont. Mech. Ther., 21 (6) (2009), 495-509.
[25] L. Gibelli, Velocity slip coefficients based on the hard-sphere Boltzmann equation, Phys. Fluids, 24 (2012), 022001.
[26] G. P. Ghiroldi and L. Gibelli, A direct method for the Boltzmann equation based on a pseudo-spectral velocity space discretization, J. Comput. Phys., 258 (2014), 568-584.
[27] X. Shan, X. Feng and H. Chen, Kinetic theory representation of hydrodynamics: A way beyond the Navier-Stokes equation, J. Fluid. Mech., 550 (2006), 413-441.
[28] Z. Li and H. Zhang, Gas kinetic algorithm using Boltzmann model equation, Comput. Fluids, 33 (2004), 976-991.
[29] V. E. Ambrus and V. Sofonea, Thermal Lattice Boltzmann models derived by Gauss quadrature using the spherical coordinate system, J. Phys. Conf. Series, 362 (2012), 1-8.
[30] R. Gatignol, Kinetic theory boundary conditions for discrete models of gases, Phys. Fluids, 20 (1977), 2022-2030.
[31] T. Inamuro, M. Yoshino and F. Ogino, A non-slip boundary condition for lattice Boltzmann simulations, Phys. Fluids, 7 (1995), 2928-2930.
[32] A. Zarghami, M. J. Maghrebi, J. Ghasemi and S. Ubertini, Lattice Boltzmann finite volume formulation with improved stability, Commun. Comput. Phys., 12 (2012), 42-64.
[33] A. Frezzotti, G.P. Ghiroldi and L. Gibelli, Solving kinetic model equations on GPUs, Comput. Fluids, 50 (2011), 136-146.
[34] G. P. Ghiroldi, L. Gibelli, P. Dagna and A. Invernizzi, Linearized Boltzmann equation: A preliminary exploration of its range of applicability, 28th International Symposium on Rarefied Gas Dynamics, 9-13 July 2012, Zaragoza, Spain, AIP Conference Proceedings American Institute of Physics, 1501 (2012), 735-741.
[35] Z. Guo, K. Xu and R. Wang, Discrete unified gas kinetic scheme for all Knudsen number flows: Low-speed isothermal case, Phys. Rev. E, 88 (2013), 033305.
[36] S. Ansumali, I. V. Karlin, S. Arcidiacono, A. Abbas and N. I. Prasianakis, Hydrodynamics beyond Navier-Stokes: Exact solution to the lattice Boltzmann hierarchy, Phys. Rev. Lett., 98 (2007), 124502.
[37] D. R. Willis, Comparison of kinetic theory analyses of linearized Couette flow, Phys. Fluids, 5 (1962), 127-135.
[38] C. E. Siewert, Poiseuille, thermal creep and Couette flow: Results based on the CES model of the linearized Boltzmann equation, Eur. J. Mech. B, 21 (2002), 579597.
[39] S. Naris and D. Valougeorgis, The driven cavity flow over the whole range of the Knudsen number, Phys. Fluids, 17 (2005), 097106.

https://doi.org/10.4208/cicp.2014.m424 Published online by Cambridge University Press